Shahrood University of Technology
Iranian Society of Mining Engineering (IRSME)
Journal of Mining and Environment (JME)
journal homepage: www.jme.shahroodut.ac.ir
THOMSON REUTERS

Numerical Modelling of Slide-Head-Toppling Failure using FEM and DEM Methods

Hassan Sarfaraz*, Alireza Bahrami and Reza Samani

School of Mining Engineering, College of Engineering, University of Tehran, Tehran, Iran

Article Info

Received 22 February 2022
Received in Revised form 12 March 2022
Accepted 17 March 2022
Published online 17 March 2022

DOI:10.22044/jme.2022.11698.2159

Keywords

Rock Slopes
Slide-head-toppling
Numerical Simulation
DEM and FEM Methods

Abstract

A common instability in the rock slopes is a toppling failure. If this type of slope failure occurs due to another kind of failure, it is considered as the secondary toppling failure. A type of secondary toppling failure is the slide-head-toppling failure. In this instability, the upper portion of the slope is toppled, and the pressure caused by the overturning of rock blocks leads to a semi-circular sliding in the soil mass at the slope toe. This instability is examined through the theoretical analysis and physical modelling. Firstly, the failure mechanism mentioned above is described. Next, the slide-head-toppling failure is studied through seven numerical simulations. The Phase2 and UDEC softwares, as the finite element and distinct element methods, respectively, are used in this work. Different kinds of slide-head-toppling failure are modelled such as the blocky, block-flexural, and flexural toppling failures. The numerical modelling results are compared with the existing physical tests and theoretical approaches. This comparison illustrates that the safety factor is underestimated due to the plane strain supposition in numerical modelling. However, the side-friction in the physical models has violated this assumption. The results obtained demonstrate that the distinct element method has an acceptable accuracy compared to the finite element method. Thus this numerical code can be used in order to examine the mentioned failure.

1. Introduction

In 1976, Goodman and Bray [1] divided the toppling failure against the main (flexural, blocky, and block-flexural) and the secondary categories based on the physical modelling and regional observations. In 1997, Adhikary et al. [2] simulated the flexural toppling instability employing a centrifuge device. Adhikary and Dyuskin [3] has also performed a new modelling utilizing a centrifuge machine on the glass and concrete samples prone to flexural toppling failure in 2007. Some works were accomplished on the numerical modelling of toppling failure in the continuum and discontinuum media [4]–[6]. Based on the principles of compatibility governing the behaviour of cantilever beams, Amini et al. [7], [8] have offered a simple methodology for flexural toppling failure, and their research works were in good agreement with the physical modelling and case study results. In 2020, Sarfaraz [9] recommended a new analytical method for flexural toppling failure using the Sarma's methodology, and he compared his theory with the Amini et al. [8] as well as the Aydan and Kawamoto approaches [10]. In 2021, he presented a simple theory for analyzing block toppling failure by applying fictitious horizontal acceleration [11]. His approach was compared with the Goodman and Bray method. By incorporating the Goodman and Bray and Aydan and Kawamoto theories, Amini et al. [12] proposed a theoretical method in order to analyze the block-flexural toppling instability. Zheng et al. [13] have presented an analysis approach for rock slopes prone to shearing and flexural toppling failure based on the limit equilibrium technique. They compared their suggested method with the physical and numerical

Corresponding author: sarfaraz@ut.ac.ir (H. Sarfaraz).

models, and the method of Aydan et al. [10]. In 2020, Sarfaraz and Amini [14] simulated the block-flexural toppling failure applying the distinct element code. Using the UDEC software as a distinct element method and the geological engineering surveys, Cai et al. [15] have investigated the toppling mechanism and deformation on a dam slope. In 2020, Kiliç and Ulamiş [16] examined the sliding and toppling mechanisms in volcanic bimrocks around Bayrakl in Izmir, and studied the relation of the blocks and the slope geometry.

For the main kind of toppling failure, the main cause of instability is the weights of rock columns. Conversely, the secondary toppling failure was stimulated by various external elements. Several studies have been published for these failures [17-28]. Sari [20] has presented a nice table in his research work for summarizing the studies related to the toppling failure types and analysis methods. A conventional kind of secondary toppling instability is a slide-head-toppling failure. In this instability, the rock blocks with the potential of toppling are located in the upper part of the slope, and the pressure caused by overturning these rock columns leads to the sliding of soil mass at the slope toe (as indicated in Figure 1). In 2018, Amini et al. [26] performed seven experimental tests for this failure, and developed an analytical solution based on the limit equilibrium method. In this research work, the physical modelling and analytical approach outcomes were evaluated using the finite and distinct element methods. The experimental models carried out by Amini et al. [26] is summarized in the following section.

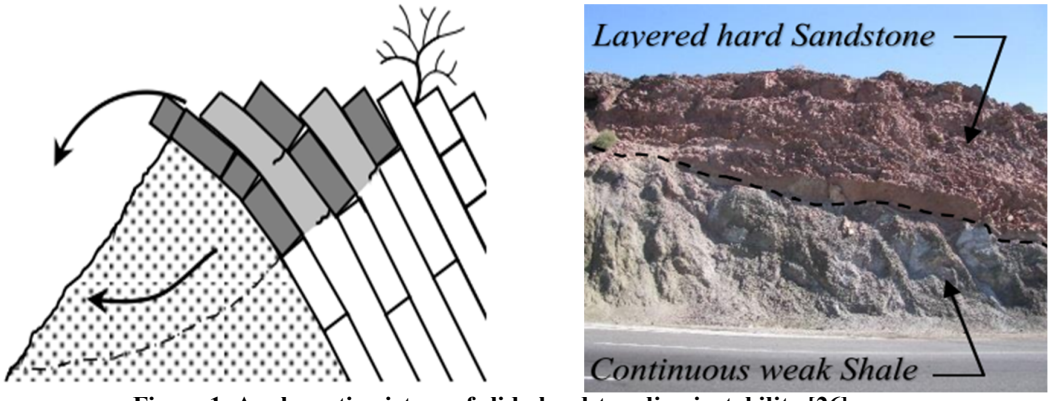

Figure 1. A schematic picture of slide-head-toppling instability [26].

2. A Review of Physical Modelling

Physical modelling is a typical procedure to examine the failure mechanism in geo-technical engineering. Amini et al. [26] have performed seven physical tests through the tilting table device indicated in Figure 2. These researchers simulated three kinds of secondary toppling, as presented in Figure 3.

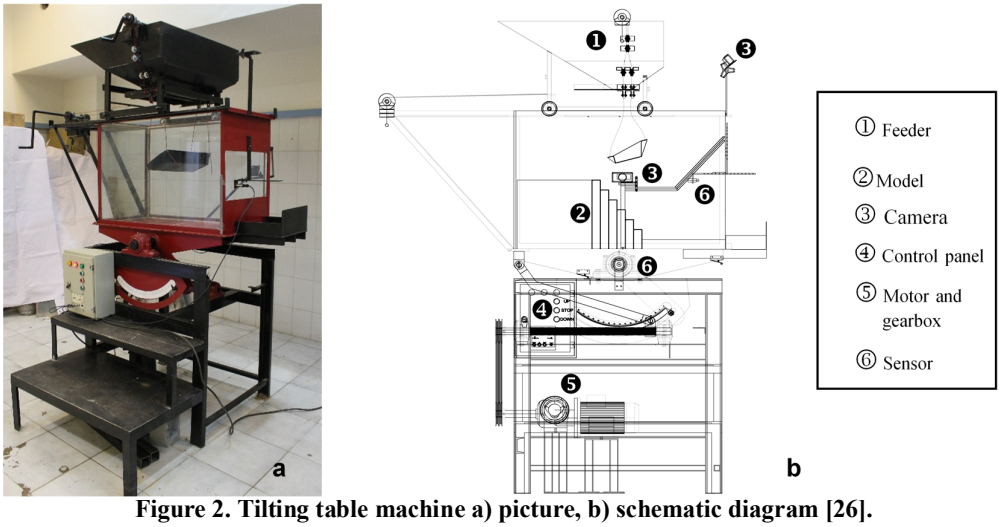

Figure 2. Tilting table machine a) picture, b) schematic diagram [26].

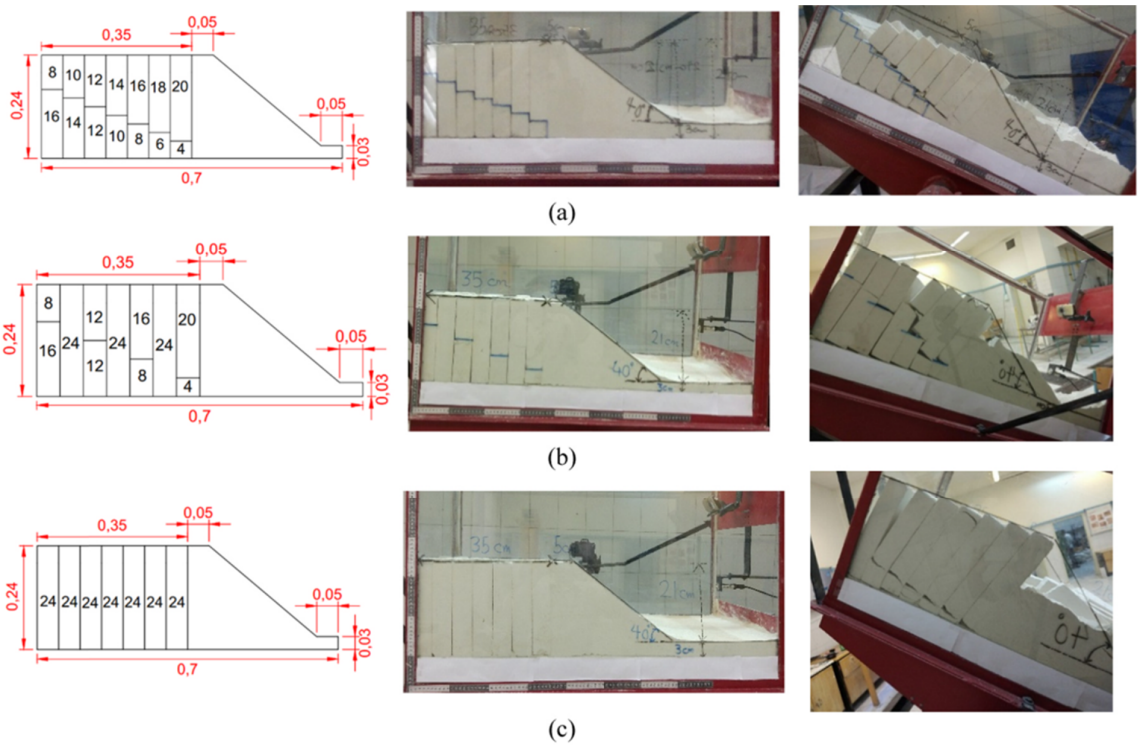

Figure 3. Physical modelling with a height of 24 cm a) blocky, b) block-flexural, c) flexural modes [26].

In the blocky toppling failure type, the fictitious cross-joints was built at the block base, and the angle of the failure surface relative to the table base was 20°. Continuous blocks were applied for modeling in the flexural toppling failure type. Due to bending, the blocks were broken at their base under tensile stress. In order to model the block-flexural toppling failure type, the partial rock columns were continuous, and the other rock blocks had cross-joint. As tilting the table, the tensile cracks were developed at the upper part of the model, and the blocks bent over soil mass. Next, a semi-circular sliding happened in the soil mass, and the blocks were suddenly toppled [26]. The physical modelling results are listed in Table 1.

Table 1. Physical model test results [26].

Model test No.	B20	B24	B30	BF20	BF24	F20	F24
Toppling mode	Block	Block	Block	Block-flexural	Block-flexural	Flexural	Flexural
Model height (cm)	20	24	30	20	24	20	24
Table inclination at failure (degree)	34.5	29	23.5	37	31.5	39	33

3. Numerical Modelling

The numerical methods are useful tools for the design and stability of project control. In a numerical model, the elements may be connected to each other, called a continuous model, and may be separated by a discontinuity, called a discrete model. The discrete models make it possible to create models of separation and slide. In this work, the physical model results are simulated using the Phase 2 and UDEC softwares, which are based on the finite element and distinct element approaches, respectively [29]. These programs are a beneficial tool to analyze the rock slope stability that has been used for the investigation of sliding and toppling failures. The capability of using this method in the analysis of discontinuous models has increased [20, 29]. In the Phase 2 code, the Goodman joint element is applied in order to examine the joints. This element can model the sliding of two joint surfaces on each other and their separation. On the other hand, the joints are evaluated with the help of the Goodman joint element, which agrees with the model to account for detachment of the joint surfaces and their sliding over each other. This characteristic allows to model the toppling failure.

Therefore, the toppling failure modelling in this software is possible. The UDEC software solves the discontinuous media problems such as the rock slopes, crack coalescence, and toppling failures in the dynamic and static conditions. The strength reduction factor (SRF) was first suggested by Zienkiewicz *et al*. in 1975 [30]. Its description of the safety factor for a slope is frequently defined as the ratio of the actual shear strength to the minimum ones of a soil or rock material required to maintain the slope equilibrium. The software performs a regular search for the strength reduction factors, starting from a unity value to the value that brings the slope to the failure verge. The critical value of this quantity found in the process is the so-called safety factor. The properties of the powder and block used in the experimental tests are given in Table 2. Furthermore, the joint properties among the blocks are illustrated in Table 3. The Mohr-Coulomb friction law was employed in the numerical modelling. The numerical models were investigated by the shear strength reduction technique. For studying the mechanism of the sliding-head-toppling instability, numerical modellings were examined based on the kind of failure at the upper region of the slope into the flexural, block, and block-flexural sections. The size of the numerical models is the same as the physical models.

Table 2. Mechanical and physical properties of powder and block [26, 31].

Element	Unit weight (kN/m^3)	Elasticity modulus (MPa)	Poison ratio	Tensile strength (kPa)	Friction angle (peak) (degree)	Friction angle (residual) (degree)	Cohesion (peak) (kPa)	Cohesion (residual) (kPa)
Solid block	21.1	10	0.27	14	35	25	100	0
Powder	16	4	0.25	0	28	22.5	0.551	0.35

Table 3. Joint elements properties [29].

Normal stiffness (MPa/m)	Shear stiffness (MPa/m)	Peak cohesion (kPa)	Residual cohesion (kPa)	Peak friction angle (degree)	Residual friction angle (degree)
100	1	0	0	32	25

3.1. Flexural toppling instability

In this failure mode, the blocks are continuous at the upper zone of the slope. Due to the bending stress, these blocks are broken and then toppled. As a result, the soil mass slides at the slope toe. As this kind of failure is sensitive to the tensile strength, the tensile stress distribution is illustrated in Figure4. According to this figure, the partial cross-sections of every block are approximately under tensile stress. In the flexural toppling instability, the failure surface determination is accompanied by many uncertainties. This plane is commonly located at the above plane perpendicular to the rock block discontinuities. This angle is estimated at 5 to 15 degrees in the experimental and analytical studies. This angle was determined in order to evaluate the accuracy of the numerical modelling outcomes, which were about 9 and 12 degrees in the Phase2 and UDEC softwares, respectively (as indicated in Figure 5 and Figure 6). SRF is achieved at 0.877 and 0.9 in the FEM and DEM approaches, respectively.

3.2. Block toppling instability

In this mode of failure, the rock columns do not withstand the tensile stresses due to the existing cross-joints, and they topple or slide due to the upstream block pressures. The shear strain contours in the Phase2 and UDEC softwares for the model of B24 are shown in Figure 7 and Figure 8, respectively. The circular failure path and shearing among joints can be seen in these figures. Besides, the rock columns overturned around their bottom, and illustrated a pure toppling. SRF is 0.894 and 0.943 in the FEM and DEM methods, respectively.

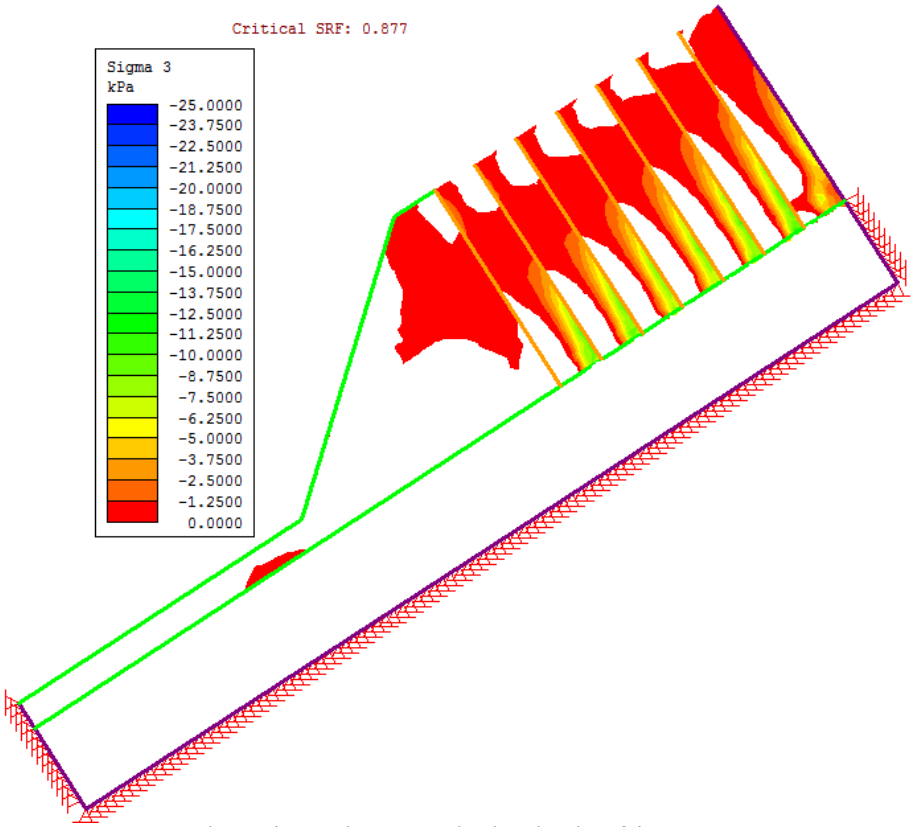

Figure 4. Tensile stress distribution in F24 model.

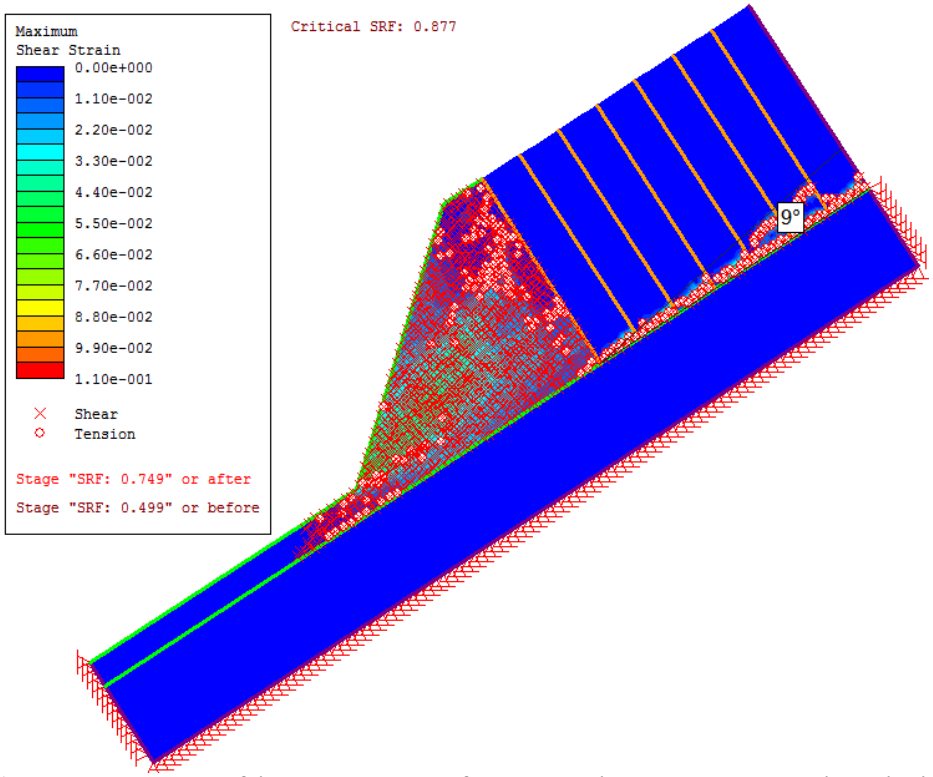

Figure 5. Angle between overall failure plane and surface perpendicular to rock mass discontinuities in F24 model in Phase2 software.

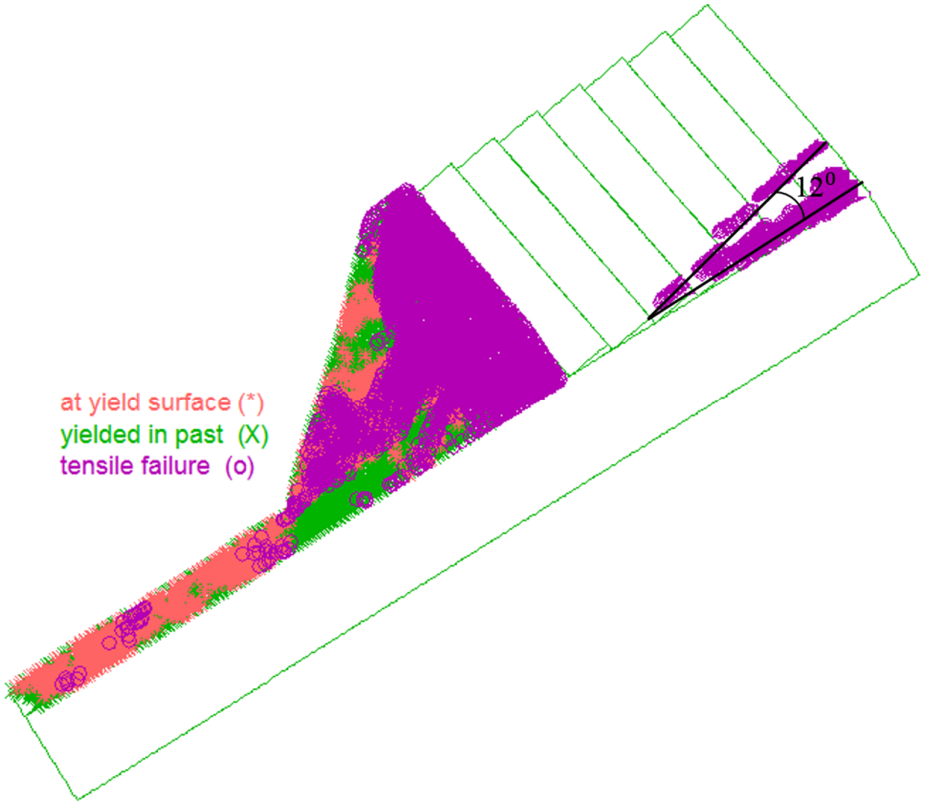

Figure 6. Angle between overall failure plane and surface perpendicular to rock mass discontinuities in F24 model in UDEC software

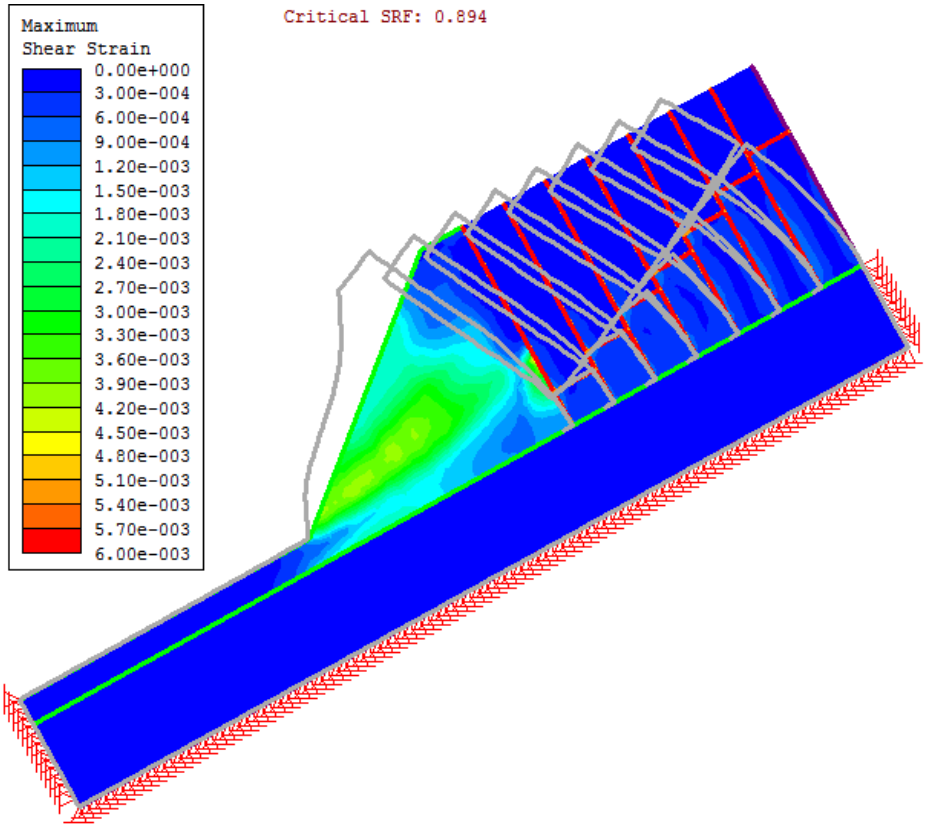

Figure 7. Shear strain contours in model of B24 using Phase2 software.

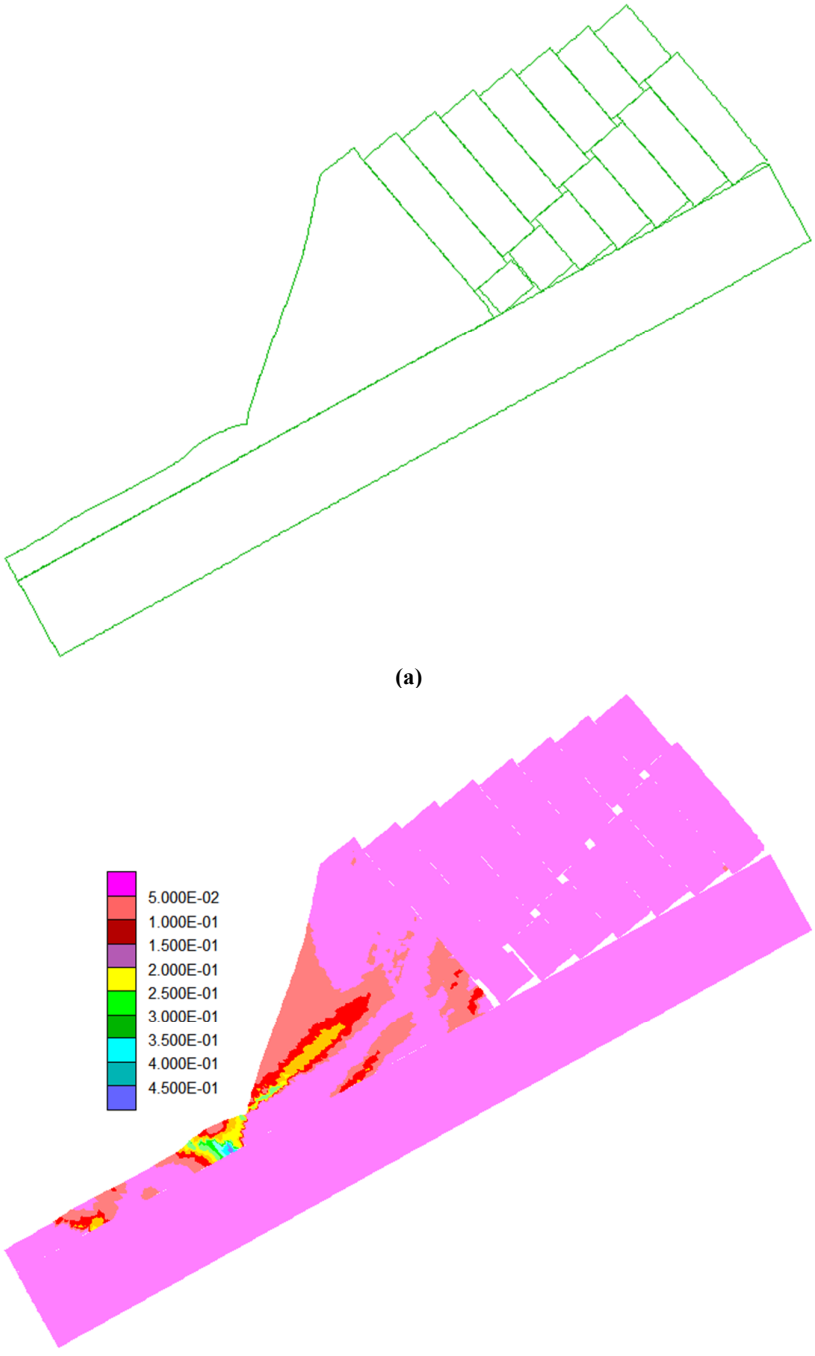

(a)

(b)

Figure 8. Numerical modelling outcomes in B24 model using UDEC software a) model plot, b) shear strain contour.

3.2. Blocky-flexural toppling instability

In this failure, the blocks are partially broken under tension stress (flexural toppling), and the other parts are separated from the cross-joints (block toppling), and then all of them are toppled together. The numerical analysis results of the BF24 model are shown in Figure 9 and Figure 10.

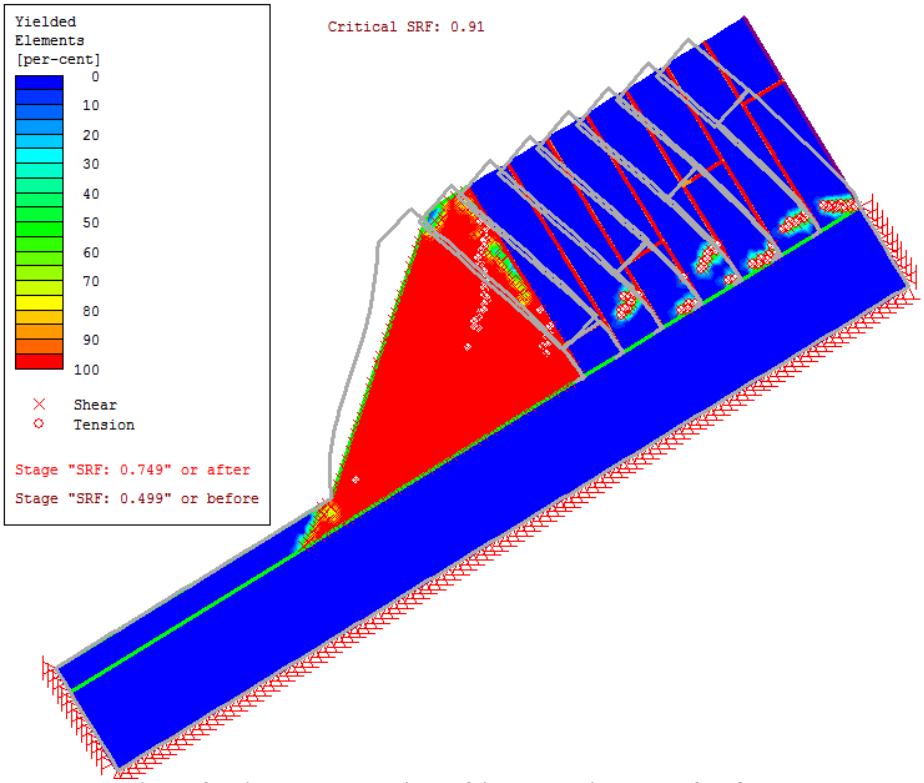

Figure 9. Yielded element in BF24 model using Phase2 software.

These figures show that the elements and joints have yielded under the shear and normal stresses. Furthermore, the overall failure plane passes via the cross-joints. SRF is 0.91 and 0.916 in the Phase2 and UDEC softwares, respectively.

4. Results and Discussion

The numerical modelling outcomes are compared with the experimental modellings in order to validate the numerical models in this section. Several diagrams and quantities are obtained in the numerical analysis, and the physical and numerical modelling results can be compared in different ways. The most proper quantity to compare these models is the critical stress reduction factor. The researchers believe that this quantity can be presumed to be equal to the factor of safety in the numerical methods [25], [30]. Since the safety factor of the experimental tests is equivalent to one at the failure moment, the critical SRF of each numerical model should also be equal to one. The safety factor (FS) of the experimental tests are compared with the stress reduction factor (SRF) of these models achieved from the numerical analysis (Table 4).

Table 4. SRF comparison in numerical modellings with experimental tests.

Models	B20	B24	B30	BF20	BF24	F20	F24
FS in physical modeling	1	1	1	1	1	1	1
SRF in UDEC software	0.9	0.943	0.966	0.865	0.916	0.814	0.9
SRF in Phase2 software	0.86	0.894	0.88	0.935	0.91	0.875	0.877
Error of UDEC software (%)	10	5.7	3.4	13.5	8.4	18.6	10
Error of Phase2 software (%)	14	10.6	12	6.5	9	12.5	12.3

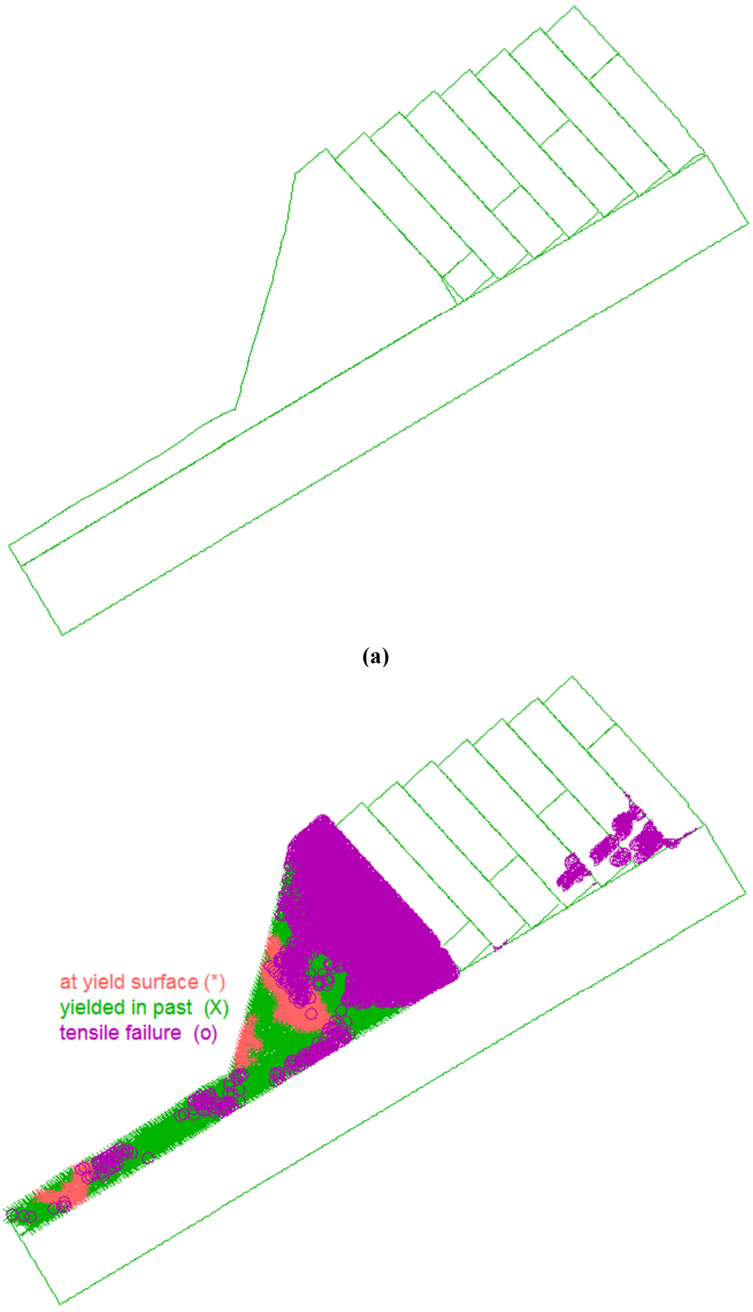

(a)

(b)

Figure 10. Yielded element in BF24 model using UDEC software a) model plot, b) plastic point plot.

As it can be seen in Table 4, the average error from the Phase2 and UDEC softwares is 10.99% and 9.94%, respectively, indicating that the results from the DEM method are more consistent with those from the FEM method, which seems reasonable due to the complex mechanism of the failure mechanism. The table inclination can also be compared between the numerical and physical tests at the moment of failure. The line perpendicular to the rock block discontinuities in the numerical models corresponds to the table inclination. This quantity can be compared between the numerical and physical model and a theoretical solution proposed by Amini et al. [26], indicated in Figure 11. This figure demonstrates an acceptable agreement between the numerical and theory outcomes. The results obtained by the distinct element method are more consistent with the results by the finite element method. The numerical modellings estimated the table

inclination to be less than the amounts measured in the experimental test in all tests. Both the numerical and physical modellings are under the plane strain conditions. However, note that the side-conditions are not completely similar in the numerical and physical models. It may be due to the side-effects in the experimental modelling, as numerical modellings are supposed to be 2D systems. In contrast, side-frictions in the experimental models lead to a 3D failure mechanism.

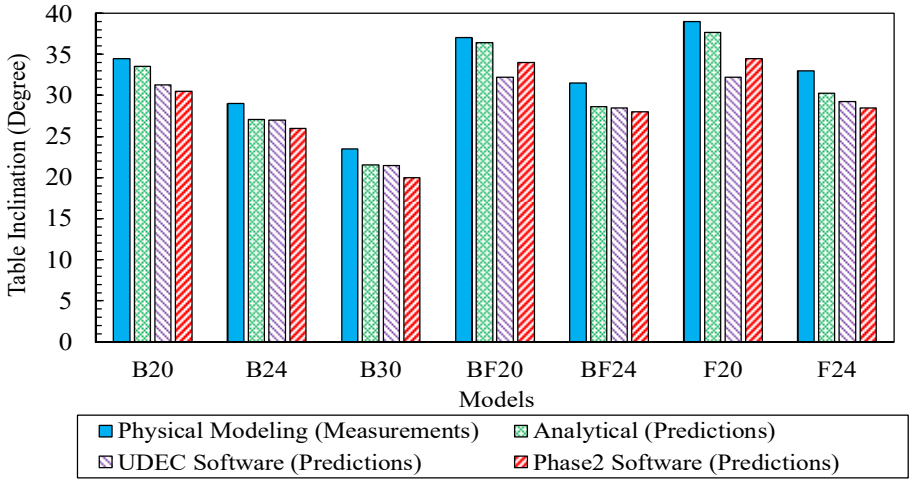

Figure 11. Comparison of numerical modelling outcomes with theoretical predictions.

5. Conclusions

This work investigated the mechanism of sliding-head-toppling instability using seven numerical modellings analyzed in the FEM and DEM methods. The outcomes can be summarized as follow:

- In the flexural toppling instability, the rock blocks are broken due to induced tensile stress and bent over of the soil mass. Consequently, the sliding failure occurs at the slope toe.
- In the block toppling instability, the blocks do not withstand tensile stresses due to the existence of cross-joints. Due to the pressure caused by the upstream blocks, they overturn or slide about the joint base, and finally, a sliding failure happens in the soil mass.
- Partial of the rock columns is broken under the induced tension stress, and the other parts are dis-jointed from the cross-joints in the blocky-flexural toppling instability. Then all the rock columns are toppled, which leads to a sliding failure at the slope toe.
- The error between the numerical modelling results with the DEM method with the physical model was approximately 9.94%, while the error between the numerical modelling results with the FEM method was approximately 11%.
- The numerical and physical modelling comparison illustrated that the safety factor was underestimated in the numerical models due to the plane strain assumption. However, the side-friction in the experimental models violated this supposition.
- This work showed that DEM had a better accuracy in evaluating the slide-head-toppling failure than FEM. Therefore, this numerical method could be used to investigate the mentioned failure.

Reference

[1]. Wyllie, D.C. and Mah, C. (2004). Rock slope engineering. CRC Press.

[2]. Adhikary, D.P., Dyskin, A.V., Jewell, R.J. and Stewart, D.P. (1997). A study of the mechanism of flexural toppling failure of rock slopes. Rock mechanics and rock engineering. 30 (2): 75-93.

[3]. Adhikary, D.P. and Dyskin, A.V. (2007). Modelling of progressive and instantaneous failures of foliated rock slopes. Rock Mechanics and Rock Engineering. 40 (4): 349-362.

[4]. Cundall, P.A. (1971). A computer model for simulating progressive, large-scale movement in blocky rock system. In Proceedings of the International Symposium on Rock Mechanics, 1971.

[5]. Pritchard, M.A. and Savigny, K.W. (1990). Numerical modelling of toppling. Canadian Geotechnical Journal. 27 (6): 823-834.

[6]. Alzo'ubi, A.K., Martin, C.D. and Cruden, D.M. (2010). Influence of tensile strength on toppling failure in centrifuge tests. International Journal of Rock

Mechanics and Mining Sciences. 47 (6): 974-982.

[7]. Majdi, A. and Amini, M. (2011). Analysis of geo-structural defects in flexural toppling failure. International Journal of Rock Mechanics and Mining Sciences. 48 (2): 175-186.

[8]. Amini, M., Majdi, A. and Aydan, Ö. (2009). Stability analysis and the stabilisation of flexural toppling failure. Rock Mechanics and Rock Engineering. 42 (5): 751-782.

[9]. Sarfaraz, H. (2020). Stability analysis of flexural toppling failure using the Sarma's method. Geotechnical and Geological Engineering. 38 (4): 3667-3682.

[10]. Aydan, Ö. and Kawamoto, T. (1992). The stability of slopes and underground openings against flexural toppling and their stabilisation. Rock Mechanics and Rock Engineering. 25 (3): 143-165.

[11]. Sarfaraz, H. (2021). An Analytical Solution for Analysis of Block Toppling Failure Using Approach of Fictitious Horizontal Acceleration. Journal of Mining Science. 57 (2): 202-209.

[12]. Amini, M., Majdi, A. and Veshadi, M.A. (2012). Stability analysis of rock slopes against block-flexure toppling failure. Rock Mechanics and Rock Engineering. 45 (4): 519-532.

[13]. Zheng, Y., Chen, C., Liu, T., Xia, K. and Liu, X. (2018). Stability analysis of rock slopes against sliding or flexural-toppling failure. Bulletin of Engineering Geology and the Environment. 77 (4): 1383-1403.

[14]. Sarfaraz, H. and Amini, M. (2020). Numerical modeling of rock slopes with a potential of block-flexural toppling failure. Journal of Mining and Environment. 11 (1): 247-259.

[15]. Cai, J.C., Ju, N.P., Huang, R.Q., Zheng, D., Zhao, W.H., Li, L. Q. and Huang, J. (2019). Mechanism of toppling and deformation in hard rock slope: a case of bank slope of Hydropower Station, Qinghai Province, China. Journal of Mountain Science. 16 (4): 924-934.

[16]. Kiliç, R. and Ulamiş, K. (2020). Toppling and sliding in volcanic bimrocks around Bayrakli (Izmir, Turkey). Journal of Mountain Science. 17 (2): 492-500.

[17]. Mohtarami, E., Jafari, A. and Amini, M. (2014). Stability analysis of slopes against combined circular–toppling failure. International journal of rock mechanics and mining sciences, 67, 43-56.

[18]. Frayssines, M. and Hantz, D. (2009). Modelling and back-analysing failures in steep limestone cliffs. International Journal of Rock Mechanics and Mining Sciences. 46 (7): 1115-1123.

[19]. Haghgouei, H., Kargar, A.R., Amini, M. and Esmaeili, K. (2020). An analytical solution for analysis of toppling-slumping failure in rock slopes. Engineering Geology, 265, 105396.

[20]. Sari, M. (2021). Secondary toppling failure analysis and optimal support design for ignimbrites in the Ihlara Valley (Cappadocia, Turkey) by finite element method (FEM). Geotechnical and Geological Engineering. 39 (7): 5135-5160.

[21]. Evans, R., Valliappan, S., Mcguckin, D. and Raja Sekar, H.L. (1981, September). Stability analysis of a rock slope against toppling failure. In ISRM International Symposium. OnePetro.

[22]. Nichol, S.L., Hungr, O. and Evans, S.G. (2002). Large-scale brittle and ductile toppling of rock slopes. Canadian Geotechnical Journal. 39 (4): 773-788.

[23]. Alejano, L.R., Veiga, M., Pérez-Rey, I., Castro-Filgueira, U., Arzúa, J. and Castro-Caicedo, Á.J. (2019). Analysis of a complex slope failure in a granodiorite quarry bench. Bulletin of Engineering Geology and the Environment. 78 (2): 1209-1224.

[24]. Alejano, L.R., Gómez-Márquez, I. and Martínez-Alegría, R. (2010). Analysis of a complex toppling-circular slope failure. Engineering Geology. 114 (1-2): 93-104.

[25]. Amini, M. and Ardestani, A. (2019). Stability analysis of the north-eastern slope of Daralou copper open pit mine against a secondary toppling failure. Engineering Geology, 249, 89-101.

[26]. Amini, M., Sarfaraz, H. and Esmaeili, K. (2018). Stability analysis of slopes with a potential of slide-head-toppling failure. International journal of rock mechanics and mining sciences, 112, 108-121.

[27]. Sarfaraz, H., Khosravi, M.H. and Amini, M. (2019). Numerical analysis of slide-head-toppling failure. Journal of Mining and Environment. 10 (4): 1001-1011.

[28]. Sarfaraz, H. (2020). A simple theoretical approach for analysis of slide-toe-toppling failure. Journal of Central South University. 27 (9): 2745-2753.

[29]. Sarfaraz, H. and Amini, M. (2020). Numerical simulation of slide-toe-toppling failure using distinct element method and finite element method. Geotechnical and Geological Engineering. 38 (2): 2199-2212.

[30]. Zienkiewicz, O.C., Humpheson, C. and Lewis, R. W. (1975). Associated and non-associated visco-plasticity and plasticity in soil mechanics. Geotechnique. 25 (4): 671-689.

[31]. Amini, M., Ardestani, A. and Khosravi, M. H. (2017). Stability analysis of slide-toe-toppling failure. Engineering Geology, 228, 82-96.

مدلسازی عددی شکست لغزش-واژگونی در رأس با استفاده از دو روش عددی المان محدود و المان مجزا

حسن سرفراز*، علیرضا بهرامی و رضا سامانی

دانشکده مهندسی معدن، دانشگاه تهران، تهران، ایران

ارسال ۲۰۲۲/۰۲/۲۲، پذیرش ۲۰۲۲/۰۳/۱۷

* نویسنده مسئول مکاتبات: sarfaraz@ut.ac.ir

چکیده:

یکی از ناپایداری‌های رایج در شیروانی‌های سنگی، شکست واژگونی می‌باشد. اگر این نوع گسیختگی به دنبال گسیختگی دیگری رخ دهد، شکست واژگونی ثانویه اطلاق می‌شود. یکی از مهم‌ترین شکست واژگونی ثانویه، شکست لغزش-واژگونی در رأس است. در این شکست، بخش فوقانی شیروانی واژگون شده و فشار ناشی از واژگونی بلوک‌های سنگی در تاج شیروانی منجر به لغزش توده خاک در پاشنه شیروانی می‌شود. این نوع شکست از طریق مدلسازی فیزیکی و روش تحلیلی بررسی شده است. در این تحقیق، ابتدا مکانیسم شکست مذکور توضیح داده می‌شود. سپس شکست لغزش-واژگونی در رأس، از طریق یک سری مدلسازی عددی مورد ارزیابی قرار می‌گیرد. از دو نرم‌افزار Phase2 و UDEC بر مبنای روش عددی المان محدود و المان مجزا استفاده شده است. انواع مختلفی از شکست لغزش-واژگونی در رأس شامل شکست بلوکی، بلوکی-خمشی و خمشی مدلسازی شده‌اند. نتایج مدلسازی عددی با مدل‌های فیزیکی موجود و روش تحلیلی مقایسه شد. مقایسه این نتایج نشان داد که در مدلسازی عددی به دلیل فرض کرنش مسطح، ضریب ایمنی کمتر از ضریب ایمنی بدست آمده در روش تحلیلی و مدلسازی فیزیکی است. نتایج به‌دست‌آمده نشان می‌دهد که روش المان مجزا از دقت قابل قبولی در مقایسه با روش المان محدود برخوردار است. بنابراین می‌توان از این کد عددی برای تحلیل شکست لغزش-واژگونی در رأس استفاده کرد.

کلمات کلیدی: شیروانی‌های سنگی، شکست لغزش-واژگونی در رأس، مدلسازی عددی، روش عددی المان محدود و المان مجزا.